

Adsorption-site determination of ordered Yb on Si(111) surfaces

C. Wigren, J. N. Andersen, and R. Nyholm

*Department of Synchrotron Radiation Research, Institute of Physics, Lund University,
Sölvegatan 14, S-22362 Lund, Sweden
and MAX-LAB, Lund University, Box 118, S-22100 Lund, Sweden*

U. O. Karlsson

Department of Physics, Material Science, Royal Institute of Technology, S-10044 Stockholm, Sweden

J. Nogami

Department of Physics, University of Wisconsin-Milwaukee, 1900 East Kenwood Boulevard, Milwaukee, Wisconsin 53201

A. A. Baski

BASF, Polymer Laboratory ZKM/T, Ludwigshafen, Germany

C. F. Quate

E. L. Ginzton Laboratory, Stanford University, Stanford, California 94305

(Received 23 July 1992; revised manuscript received 28 December 1992)

Low-energy-electron-diffraction (LEED), scanning-tunneling-microscopy (STM), and photoelectron-spectroscopy measurements have been performed on the ordered submonolayer surface reconstructions of Yb on Si(111). Two of these reconstructions, namely, 3×1 and 2×1 , have been studied in detail. STM and LEED revealed that what was considered to be the 3×1 reconstruction is actually a 3×2 reconstruction. By combining STM and photoelectron-spectroscopy results from the 3×2 and 2×1 reconstructions, we conclude that the Yb atoms are adsorbed in bridge sites.

INTRODUCTION

The mechanisms behind the formation of metal-induced surface reconstructions on semiconductor surfaces, such as the Si(111) surface, are still not fully understood. The geometrical structures are in many cases still under discussion. A class of surface structures that is believed to be known is the $(\sqrt{3}\times\sqrt{3})R\ 30^\circ$ structures formed by one-third monolayer (ML) [1 ML=1 atom per Si(111) surface unit mesh] of the trivalent group-III elements (B,Al,Ga,In,...) on Si(111). The atoms of group III have three valence electrons and, in a simplified picture, energy minimization is obtained by completely eliminating dangling bonds simply by placing the atoms in a threefold site on an unreconstructed Si(111) surface. It has been shown that the group-III elements, except for B, prefer to be adsorbed in the threefold site directly above the second Si-layer atoms (T_4) rather than in the site above the fourth Si-layer atoms (H_3).¹ If instead, a divalent atom is deposited on the Si(111) surface the situation changes completely. A complete elimination of all dangling bonds can no longer be achieved in a H_3 or a T_4 site and naively one might believe that a twofold bridge site would be the most favorable position for a divalent atom. An example where a bridge site has been suggested for a divalent metal adsorbed on Si(111) is the Ca/Si(111) surface.²

The divalent metal Yb adsorbed on Si(111) shows several ordered surface reconstructions. In the present

investigation two of these ordered structures, namely, 3×1 and 2×1 , have been studied in detail by photoelectron spectroscopy (PES) and scanning tunneling microscopy (STM). From the combined PES and STM results structural models with the Yb atoms adsorbed in bridge sites are found to be the most plausible.

EXPERIMENT

The measurements were performed in two different chambers, one equipped with a commercial STM instrument³ at the Ginzton Laboratory, Stanford, USA, and the other equipped with a double-pass cylindrical-mirror analyzer for the recordings of photoelectron spectra at MAX-LAB, Lund University, Sweden. Both chambers were equipped with low-energy-electron-diffraction (LEED) optics. The base pressure in the chambers was below 1×10^{-10} torr. The Si(111) wafers were cleaned by flashings to $\sim 1150^\circ\text{C}$ and then slowly cooled down or by chemical etching⁴ prior to the insertion in the vacuum chamber in which case the thin oxide formed in the etching procedure could be removed by heating to $\sim 900^\circ\text{C}$. Sample heating was done by electron bombardment from the back side of the crystal or by Ohmic heating. Sample cleanness was checked with LEED and STM which both showed excellent 7×7 structures characteristic of clean Si(111) surfaces. Surface cleanness was also checked with PES which showed characteristic surface components in core-level and valence-band spectra^{5,6} for the clean surfaces. A modified SX700 plane grating monochromator⁷

at the synchrotron radiation facility at MAX-LAB provided the monochromatized photons. Two types of Yb evaporators were used, one in which Yb was evaporated from an outgassed Yb bead inside a tungsten wire basket. The other type consisted of a Yb bead inside a tantalum tube heated by radiation from a tungsten filament. A quartz-crystal thickness monitor measured the evaporation rate which typically was between 0.1–1 ML/min. During evaporation the pressure was kept in the low 10^{-10} -torr region. Ordered LEED patterns were obtained either by evaporating Yb onto warm ($\sim 500^\circ\text{C}$) substrates or by annealing the samples after the evaporations were completed.

RESULTS AND DISCUSSION

Upon Yb deposition onto a warm ($\sim 500^\circ\text{C}$) Si(111) substrate, or onto the substrate at room temperature followed by annealing, several submonolayer Yb-induced surface reconstructions appear. Yb atoms can have different valency in different environments. For Yb the valency can be conveniently measured by PES of the Yb 4*f* level since the 4*f* levels of divalent and trivalent Yb have a different appearance and are well separated in binding energy (see, e.g., Ref. 8). It was found that Yb is completely divalent in all submonolayer reconstructions. Furthermore, since no Fermi edge is seen in valence-band spectra from these reconstructions it is concluded that all these surfaces are semiconducting. Earlier measurements^{8,9} have shown that the Yb atoms are mixed valent in the bulk of Yb silicides, that is, signals from both trivalent and divalent Yb are seen in the PES of the Yb 4*f* level. From the absence of a trivalent signal in the spectra from the submonolayer reconstructions and the knowledge¹⁰ that the divalent configuration is stabilized at the surface we conclude that the Yb atoms adsorb on the surface. Furthermore, this is in agreement with a previous ion scattering study.¹¹ The ordered patterns observed in LEED are, in order of increasing coverage, 3×1 with $\frac{1}{2}$ -order streaks (Fig. 1), 5×1 , 7×1 , and

2×1 .¹¹ Similar series of metal-induced surface reconstructions have also been observed for other divalent atoms such as Ca (Refs. 2 and 12) and Sm (Ref. 13) adsorbed on Si(111). The Yb-Si(111) 3×1 structure has a remarkable feature. Besides sharp intense 3×1 spots on a low background, continuous lines were observed at $\frac{1}{2}$ -order positions in the LEED pattern, as sketched in Fig. 1. The most intense lines were generally observed from the surfaces of the highest quality. These $\frac{1}{2}$ -order lines are an indication of one-dimensional disorder, as will be discussed below. The other reconstructions do not show any sign of such one-dimensional disorder and the 2×1 pattern has very sharp spots on a low background. The quality of the 5×1 and 7×1 patterns are not as high as the quality of the 3×1 and 2×1 patterns and the 7×1 reconstruction is especially difficult to produce over large areas which is probably the reason why it was not observed in earlier work.¹¹

Figure 2 shows an STM picture from a preparation in which a 7×7 pattern, characteristic of clean Si(111) surfaces, is seen in LEED together with weak 3×1 spots. A boundary between a 7×7 and a 3×1 domain is seen in the image. The image clearly shows that the 3×1 phase consists of rows in the $\langle 1\bar{1}0 \rangle$ directions. The separation between the rows is $3a$, where $a = 3.84 \text{ \AA}$ is the unit distance on an unreconstructed Si(111) surface. These rows

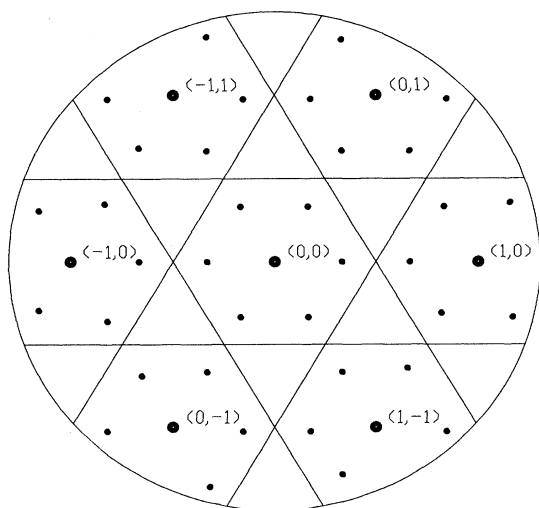


FIG. 1. A sketch of the 3×1 LEED pattern with half-order streaks.

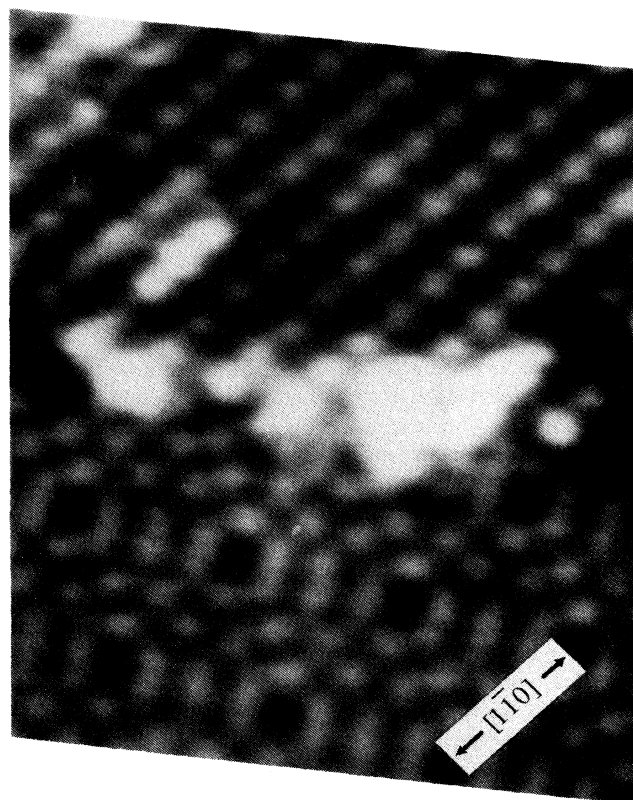


FIG. 2. An STM image showing a domain boundary between a 7×7 and a 3×1 domain. Notice the structure in the $[1\bar{1}0]$ direction which has the periodicity $2a$, where $a = 3.84 \text{ \AA}$ is the length of the Si surface lattice vector.

consist of protrusions separated by $2a$. No correlation exists between the position of the protrusions in adjacent rows, and the structure may be described as a mixture between a 3×2 and a $c(6 \times 2)$ structure. Such one-dimensional disorder gives rise to the observed half-order streaks in the 3×1 LEED pattern [cf. Au/Si(111) 5×2 (Ref. 14)]. From now on, this structure will be denoted as 3×2 . Height measurements showed that the height of the protrusions in the 3×2 structure over the surrounding 7×7 structure is 1.1 ± 0.2 Å. If corrections are made for the adatom height in the 7×7 structure,¹⁵ this results in a protrusion height above an unreconstructed Si substrate of 2.2 ± 0.3 Å. Using the covalent radius of Si atoms (1.17 Å) and the ionic radius of divalent Yb (1.94 Å), one finds a difference in height between the cores of the Yb and the Si surface atoms in the threefold, bridge, and on top adsorption sites of 2.2, 2.4, and 3.1 Å, respectively. Thus the height difference between the protrusions and the 7×7 surrounding from the STM measurements does not contradict a structure where the protrusions correspond to Yb atoms adsorbed on an unreconstructed Si(111) substrate. The Yb/Si(111) 3×2 structure is thereby different from the 3×1 structures formed by monovalent atoms (i.e., Ag and the alkali metals) on Si(111) in which the 3×1 structure clearly involves a rearrangement of the substrate Si rather than simple metal-adatom adsorption.¹⁶ Since valence-band spectra show that the submonolayer Yb/Si(111) surfaces are semiconducting, there has to be an even number of electrons in the surface unit mesh. It is not obvious how this requirement can be fulfilled in a Yb-induced 3×1 reconstruction and it is thus satisfying to find that the 3×1 reconstruction¹¹ is actually a 3×2 reconstruction. In a 3×2 surface unit mesh an even number of electrons in the surface unit mesh can be obtained in a simple structure where the Yb atoms adsorb on an unreconstructed Si substrate.

At a Yb coverage three times that of the 3×2 structure STM shows a structure consisting of rows separated by $2a$ and LEED shows a distinct 2×1 pattern. A Yb coverage for the 2×1 surface three times that of the 3×2 surface is consistent with models having one Yb atom per surface unit mesh in the 2×1 and the 3×2 structures. The coverage of 0.5 ML is also consistent with the readings of a quartz-crystal thickness monitor. In a structural model with one Yb atom per 2×1 surface unit mesh the Yb atoms are quite densely packed which explains why only a very small corrugation could be seen along the rows in STM.

The STM data give us some information about the metal registry with the underlying Si bilayer from examination of phase boundaries between the 3×2 and 7×7 images as in Fig. 2. Based on the dimer-adatom-stacking fault model¹⁷ for the 7×7 structure it is possible to determine the position of the T_4 sites in the image by using guiding lines through the corner holes and adatoms seen in the 7×7 part of the image. From such an analysis it is possible to exclude H_3 and on top adsorption sites for the Yb atoms [assuming that the protrusions seen in the image are Yb atoms adsorbed on a truncated Si(111) surface]. However, the bridge sites are very close to the T_4

sites and it is not possible to distinguish between the bridge and T_4 sites as adsorption sites for the Yb atoms from the analysis of the STM images. This problem may be addressed with PES. The core-level binding energies are sensitive to the chemical surroundings of the atoms and differences in Yb-Si coordination numbers should be possible to extract from PES. It should, for instance, be possible to distinguish between Si atoms that are singly and doubly coordinated to Yb. In the latter case the Yb-induced Si $2p$ binding-energy shift should be approximately twice as large as in the former case.¹⁸

Figure 3 shows two possible adsorption site models for the 3×2 and 2×1 structures. In the first model [Figs. 3(a) and 3(b)] the Yb atoms are positioned in T_4 sites and in the second model a bridge adsorption site is proposed. For the 2×1 models, a major difference exists between the bridge site model and the T_4 site model. In the bridge model, Fig. 3(d), all surface Si atoms bond to one Yb atom, whereas in the T_4 model [Fig. 3(b)] surface Si atoms bonded to one and to two Yb atoms are present in equal numbers. It is possible to distinguish between the bridge and T_4 adsorption site models with PES since Si atoms that are singly and doubly coordinated to Yb should have different Si $2p$ binding-energy shifts. The Si $2p$ binding-energy shift from Si atoms that are singly coordinated to Yb can be obtained from the Si $2p$ spectra from the 3×2 surface since, irrespective of what model is used, the 3×2 structure only contains Si surface atoms that are singly coordinated to Yb.

In Si $2p$ spectra, Fig. 4, from the 3×2 and 2×1 structures two main (spin-orbit-split) components are ob-

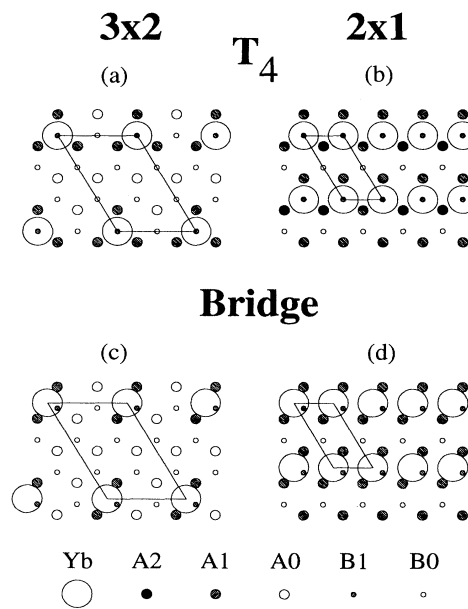


FIG. 3. Structural models of the 3×2 and 2×1 Yb surface structures on the Si(111) surface. In (a) and (b) the Yb atoms are placed in T_4 sites and in (c) and (d) the Yb atoms are placed in bridge sites. A_0 , A_1 , and A_2 are Si atoms in the top layer coordinated to zero, one and two Yb atoms, respectively, B_0 and B_1 are Si atoms in the second Si layer.

served. It is immediately seen that the binding-energy difference between the components is approximately equal for the 3×2 and the 2×1 surfaces. In order to vary the escape depth of the emitted photoelectrons, making possible a separation between bulk and surface contributions, the spectra were recorded at different photon energies. The most surface-sensitive spectra were obtained using a photon energy of 130 eV. From the photon-energy dependence the high binding-energy component is identified as a bulk component. A clear difference between the spectra from the two surfaces is that the intensity of the surface-shifted component increases considerably when going from the 3×2 to the 2×1 surface. This increase in intensity makes it possible to assign this surface component to Si atoms with Yb neighbors; this is also what is expected if the sign of the Yb-induced shift is estimated theoretically.¹⁹ If the Yb atoms are assumed to adsorb in high symmetry sites and with the adsorption site being the same in the 2×1 and 3×2 structures, then the similar shifts immediately show that the Yb atoms adsorb in bridge sites, since these models are the only high symmetry models, not excluded by the STM data, that give the same Yb-induced binding-energy shift of the Si $2p$ levels in both the 3×2 and 2×1 structures.

To extract further information decompositions of the spectra in Fig. 4 were made. Spin-orbit-split Voigt functions were used with the Lorentzian full width at half

maximum (FWHM) fixed at 0.11 eV. The Gaussian FWHM was the same for all components but was allowed to vary until optimum fits were obtained. The optimum Gaussian FWHM was 0.28 eV. The main features in the spectra are a bulk component (*B*) and a surface component (*S1*) shifted 0.47 eV towards lower binding energy. Fittings using only these two components were impossible if photon-energy-dependent shifts and/or asymmetries of the components were to be avoided. To avoid these effects in the results of the fittings two additional surface components, *S2* and *S3*, were introduced on both sides of the bulk component (shifted by 0.2 eV). The absence of *S2* led to a photon-energy-dependent shift between the bulk and the *S1* component. This effect was especially noticeable in fittings of the spectra from the 2×1 surface but was not as strong in fittings of spectra from the 3×2 surface where reasonable fits could be obtained without *S2*. In fittings of spectra from the 3×2 and the 2×1 reconstructions the *S3* component was needed in order not to get a photon-energy-dependent asymmetric line shape of the bulk component. The absolute positions and intensities of *S2* and *S3* are quite sensitive to the linewidths and are therefore rather uncertain.

From the direct inspection of the spectra it was concluded that the Yb atoms adsorb in bridge sites. These conclusions were based on the similar Yb-induced shift in spectra from the 3×2 and 2×1 surfaces. This is further verified in the decomposition where, within the accuracy of the curve fittings, the shift of *S1* relative the bulk component is found to be equal in the 3×2 and 2×1 spectra. The results of the curve fittings also show that the intensity of *S1* differs almost by a factor of 2 between the 3×2 and 2×1 spectra and since the Yb coverage increases between the 3×2 and 2×1 reconstructions this shows that the *S1* component is Yb related. The results of the fittings of the Si $2p$ spectra from the 3×2 and 2×1 reconstructions thus lead to the same conclusions as were obtained from a direct inspection of the spectra, i.e., that the Yb atoms adsorb in bridge sites in the 3×2 and 2×1 Yb-induced reconstructions of Si(111). However, there are a few details in the spectra that need a more thorough discussion.

In the bridge models the number of Si atoms bonding to one Yb atom (the *A1* atoms in Fig. 3) increases by a factor of 3 in going from the 3×2 reconstruction to the 2×1 reconstruction. However, the intensity of the *S1* component of the Si $2p$ spectra, that has been attributed to these atoms, does not increase by the same amount (it only increases by a factor of 2) and is thus slightly ($1.5\times$) too large in the spectra from the 3×2 surface. This might be due to an overlap of two components contributing to the intensity of *S1*. Valence-band spectra have shown that the 3×2 reconstruction is semiconducting and therefore no half-filled dangling bonds should exist in the surface. However, there are four Si atoms in the surface unit mesh not bonding to Yb (the *A0* atoms in Fig. 3). The semiconducting properties of the surface mean that these atoms have to interact with each other in order to eliminate the half-filled dangling bonds on these atoms. This interaction could be in the form of charge transfer from one Si dangling bond to another. Such a charge

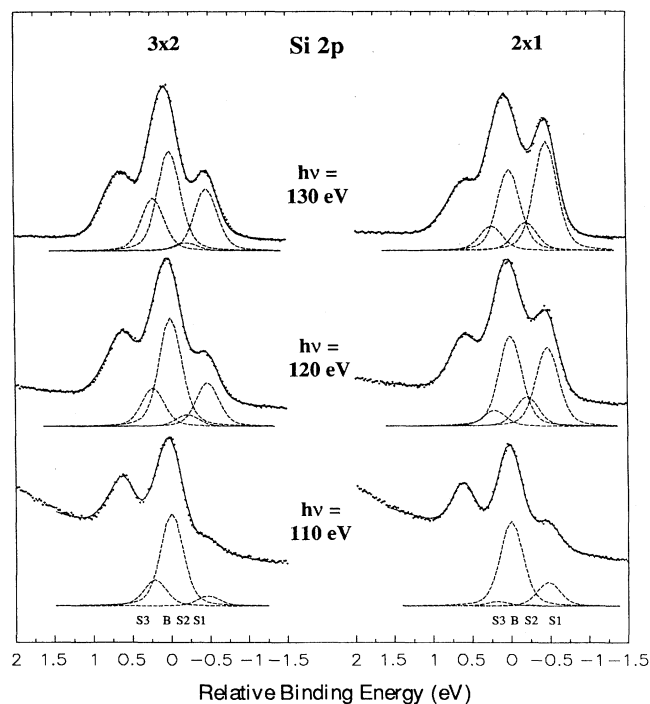


FIG. 4. Si $2p$ core-level spectra (dots) from the Yb-induced 3×2 and 2×1 structures recorded at three photon energies. The full lines show fits to the data using four spin-orbit-split components. The dashed lines show the individual components (for clarity, only the $2p_{3/2}$ peaks of the model functions are shown).

transfer can result in a Si 2*p* binding-energy shift, for half the unbonded Si atoms, of the same magnitude as the Yb-induced binding-energy shift.^{18,20,21} Another contribution to the discrepancy between the estimated relative intensity for *S*1 based on the bridge models in Fig. 3 and the measured intensities could be diffraction effects.

The decomposition of the Si 2*p* spectra from the Yb-induced 3×2 and 2×1 surface reconstruction revealed three surface components. In interpretations of the spectra where only the type and number of nearest neighbors affect the core-level binding energy, the number of surface components found in the decomposition does not seem compatible with the models proposed in Fig. 3. However, it has recently been realized that the core levels of Si atoms in the second Si(111) surface layer are shifted relative to those of the bulk Si atoms. This second-layer effect has been seen in two different systems, the Al-Si(111)(√3×√3)*R* 30° (Ref. 22) and the clean Si(111)2×1 (Ref. 20) surfaces. In both of these cases the second-layer core-level shift was about 0.2 eV towards higher binding energy, that is, the same shift as is observed for *S*3 in the present case. Therefore it is reasonable to assume that second-layer Si atoms contribute to the intensity of *S*3. A remarkable behavior of *S*3 is that it decreases drastically in intensity when going from 3×2 to the 2×1 and instead the intensity of the *S*2 component is increasing. This might indicate that both these components are from the second-layer Si. If the result of the curve fittings is put in relation to the bridge site models for the 3×2 and 2×1 surfaces then the natural assignment would be that the *S*2 component is due to Si atoms of *B*1 type in the second layer and *S*3 is due to the Si atoms of *B*0 type (see Fig. 3). In the Yb-Si(111)2×1 surface the number of *B*1 atoms is much higher than in the 3×2 surface which is reflected in the increased intensity of *S*2. This core-level shift would then be due to a second nearest-neighbor effect; such an effect has, for instance, been seen in the *B*-

Si(111)(√3×√3)*R* 30° surface.²³ Part of the decrease in intensity of the *S*3 component between spectra from the 3×2 and 2×1 reconstruction could of course also be attributed to Si atoms in the first Si surface layer contributing to the *S*3 intensity in the spectra from the 3×2 reconstruction but not in spectra from the 2×1 reconstruction. As discussed above half of the Si atoms in the first layer not bonding to Yb in the 3×2 structure may contribute to the intensity of *S*1. The other half of these atoms may contribute to the intensity of *S*3 and since no such atoms are present in the 2×1 structure this would result in a decrease of the *S*3 intensity.

SUMMARY

It has been shown that PES combined with STM and LEED can provide information on the detailed bonding of adsorbed atoms on semiconductor surfaces. The adsorption of Yb on the Si(111) surface has been studied and it has been shown that the divalent Yb atoms adsorb in bridge sites rather than in the *H*₃ site proposed in Ref. 11. This is consistent with an intuitive expectation based upon experiences from the adsorption of trivalent metals at low coverage. In these cases the adsorbed trivalent atoms are found to adsorb in threefold sites in which the three valence electrons of the adsorbed atom can saturate three Si dangling bonds. Similarly, a divalent atom could in a twofold site, i.e., in a bridge site, saturate two Si dangling bonds.

ACKNOWLEDGMENTS

The authors would like to acknowledge financial support from the Swedish Natural Science Research Council.

¹R. I. G. Uhrberg and G. V. Hansson, *Crit. Rev. Solid State Mater. Sci.* **17**, 133 (1991).

²M. A. Olmstead, R. I. G. Uhrberg, R. D. Bringans, and R. Z. Bachrach, *J. Vac. Sci. Technol.* **B4**, 1123 (1986).

³Park Scientific Instruments, Sunnyvale, CA 94089.

⁴A. Ishizaka and Y. Shiraki, *J. Electrochem. Soc.* **133**, 666 (1986).

⁵F. J. Himpsel, P. Heimann, T.-C. Chiang, and D. E. Eastman, *Phys. Rev. Lett.* **45**, 1112 (1980).

⁶F. J. Himpsel, D. E. Eastman, P. Heimann, B. Reihl, C. W. White, and D. M. Zehner, *Phys. Rev. B* **24**, 1120 (1981); T. Yokotsuka, S. Kono, S. Suzuki, and T. Sagawa, *Solid State Commun.* **39**, 1001 (1981).

⁷R. Nyholm, S. Svensson, J. Nordgren, and A. Flodström, *Nucl. Instrum. Methods Phys. Res. A* **246**, 267 (1986).

⁸C. Wigren, J. N. Andersen, R. Nyholm, and U. O. Karlsson, *J. Vac. Sci. Technol. A* **9**, 1942 (1991).

⁹A. Iandelli, A. Palenzona, and G. Olcese, *J. Less-Common Met.* **64**, 213 (1979); I. Abbati, L. Braicovich, C. Carbone, J. Nogami, I. Lindau, I. Iandelli, G. Olcese, and A. Palenzona, *Solid State Commun.* **62**, 35 (1987).

¹⁰B. Johansson and N. Mårtensson, in *Handbook on the Physics and Chemistry of Rare Earths*, edited by K. A. Gschneidner, Jr., L. Eyring, and S. Hüfner (North-Holland, Amsterdam, 1987), Vol. 10, p. 361.

¹¹J. Kofoed, I. Chorkendorff, and J. Onsgaard, *Solid State Commun.* **52**, 283 (1984).

¹²J. F. Morar (private communication).

¹³C. Wigren, J. N. Andersen, R. Nyholm, M. Götelid, M. Hammar, C. Törnevik, and U. O. Karlsson (unpublished).

¹⁴H. Lipson and K. E. Singer, *J. Phys. C* **7**, 12 (1974).

¹⁵R. M. Feenstra and M. A. Lutz, *Phys. Rev. B* **42**, 5391 (1990).

¹⁶K. J. Wan and J. Nogami (unpublished).

¹⁷K. Takayanagi, Y. Tanishiro, M. Takahashi, and S. Takahashi, *J. Vac. Sci. Technol. A* **3**, 1502 (1985); *Surf. Sci.* **164**, 367 (1985).

¹⁸F. J. Himpsel, B. S. Meyerson, F. R. McFeely, J. F. Morar, A. Taleb-Ibrahimi, and J. A. Yarmoff, in *Photoemission and Absorption Spectroscopy of Solids and Interfaces with Synchrotron Radiation*, Proceedings of the International School of Physics "Enrico Fermi," Course CVIII, Varenna, 1988, edited by M. Campagna and R. Rosei (North-Holland, Amsterdam, 1990).

- ¹⁹M. del Giudice, J. J. Joyce, and J. H. Weaver, *Phys. Rev. B* **36**, 4761 (1987).
- ²⁰J. C. Woicik, P. Pianetta, and T. Kendelewicz, *Phys. Rev. B* **40**, 12 463 (1989).
- ²¹E. Landemark, C. J. Karlsson, Y.-C. Chao, and R. I. G. Uhrberg, *Phys. Rev. Lett.* **69**, 1588 (1992).
- ²²J. N. Andersen, C. Wigren, and U. O. Karlsson, *J. Vac. Sci. Technol. B* **9**, 2384 (1991).
- ²³J. E. Rowe, G. K. Wertheim, and D. M. Riffe, *J. Vac. Sci. Technol. A* **9**, 1020 (1991).

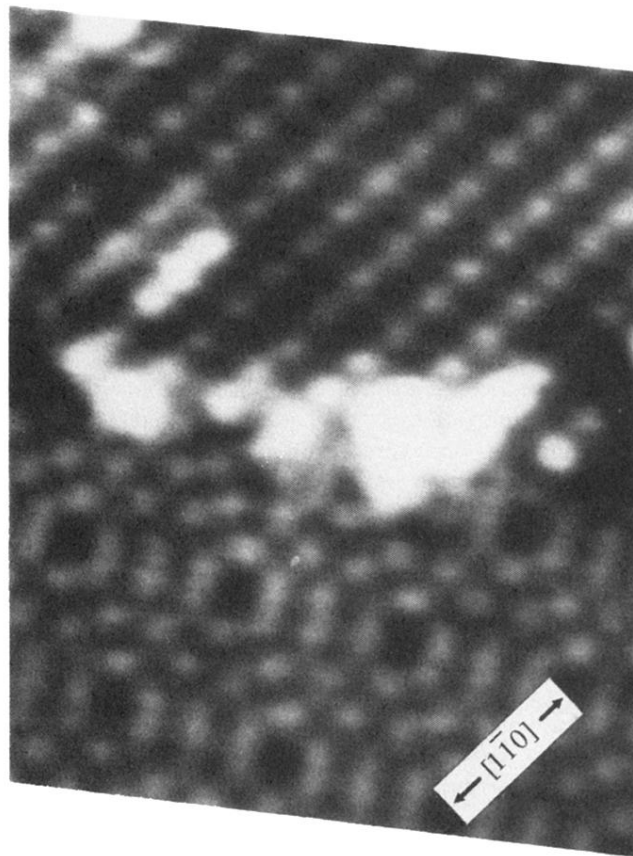


FIG. 2. An STM image showing a domain boundary between a 7×7 and a 3×1 domain. Notice the structure in the $[1\bar{1}0]$ direction which has the periodicity $2a$, where $a = 3.84 \text{ \AA}$ is the length of the Si surface lattice vector.